

Fabrication and near-room temperature transport of patterned gold cluster structures

L. Clarke and M. N. Wybourne^{a)}

Department of Physics, University of Oregon, Eugene, Oregon 97403

Mingdi Yan, S. X. Cai, L. O. Brown, J. Hutchison, and J. F. W. Keana

Department of Chemistry, University of Oregon, Eugene, Oregon 97403

(Received 28 May 1997; accepted 28 July 1997)

Ligand stabilized metal clusters are becoming of considerable interest for possible nanoscale electronics applications. In this article, we report the fabrication and near-room temperature electrical transport properties of structures made from the gold-cluster material $\text{Au}_{55}[\text{P}(\text{C}_6\text{H}_5)_3]_{12}\text{Cl}_6$. While other strategies to produce cluster arrays have been reported, this work is the first to use electron-beam lithography to laterally define the structures. We compare the current–voltage characteristics of nonpatterned and patterned structures, and show that in both cases the nonlinear behavior observed is consistent with Coulomb blockade dominated transport. We argue that charging of individual Au_{55} cores is responsible for the effects observed. © 1997 American Vacuum Society. [S0734-211X(97)01406-6]

I. INTRODUCTION

The interaction between charged particle beams and organometallics is a well-established technology to produce directly written metal features. For example, platinum structures have been deposited by the reaction between an ion-beam and an organometallic gas,¹ and palladium structures have been produced by both ion- and electron-beam exposure of palladium-acetate films.^{2,3} Metal-cluster compounds exposed to charged particle beams have also been investigated for metal structure production. After exposure, the structures are usually highly resistive. To lower the resistivity a postexposure annealing process is used to remove organic material trapped in the exposed structures. One metal-cluster material that has been studied for direct writing applications under ion- and electron-beam exposure is dodeca(triphenylphosphine)hexa(chloro)pentaconta gold, $\text{Au}_{55}[\text{P}(\text{C}_6\text{H}_5)_3]_{12}\text{Cl}_6$.^{4,5}

An interesting and potentially useful aspect of $\text{Au}_{55}[\text{P}(\text{C}_6\text{H}_5)_3]_{12}\text{Cl}_6$ for nanoscale electronics based on Coulomb charging^{6,7} is the smallness of the gold core which has an estimated radius, r , of 0.7 nm.⁷ The gold core is stabilized by a triphenylphosphine ligand sphere of radius 1.05 nm.⁷ The size of the core radius suggests that an isolated Au_{55} will have an extremely low geometrical capacitance, $C = 4\pi\epsilon\epsilon_0r$, and a Coulomb charging energy, $E_c = e^2/2C$, greatly exceeding the thermal energy at room temperature, kT_{RT} . Under these conditions, energy E_c is required to place an extra electron onto the core. This energy is provided by an external potential, thus no net charge transfer can occur until sufficient bias is applied. This phenomenon is referred to as Coulomb blockade. Scanning electron microscopy (SEM) experiments have been used to investigate Coulomb charging effects in isolated Au_{55} clusters at room temperature (RT).⁸ Coulomb blockade effects are expected to influence the

transport properties of an array of metal cores separated from each other by a dielectric that provides an intercore tunnel resistance, R_T , greater than the quantum resistance h/e^2 . These blockade effects will remain up to RT so long as the additional capacitance due to the presence of other cores, and a ground plane is not large enough to reduce the charging energy below kT_{RT} . Under the conditions for blockade, structures containing many clusters isolated from each other by tunnel barriers are anticipated to have nonlinear current–voltage (I – V) characteristics similar to those reported for tunnel junction arrays and single electron transistors operating at low temperature.^{9,10} Such arrays are expected to exhibit coherent electron tunneling effects that may be observed in the presence of a phase locking radio frequency (rf) field. These transport features suggest that metal cluster systems may find future application in nanoelectronic devices^{10,11} that operate at RT.

Several strategies have been reported for the fabrication of three-, two-, and one-dimensional arrays of metal clusters.^{7,12–14} In this article we present electrical transport characteristics of organometallic structures made from $\text{Au}_{55}[\text{P}(\text{C}_6\text{H}_5)_3]_{12}\text{Cl}_6$. We report two different realizations, one patterned by electron-beam irradiation, the other nonirradiated. In neither case was a postfabrication anneal used to remove organic material. We demonstrate that the near-room temperature transport properties of both realizations have features consistent with the charging of individual Au_{55} cores.

II. EXPERIMENT

The gold cluster material was synthesized following the procedure of Schmid.¹⁵ Various purification procedures were used to remove monomer material. Solutions of the gold cluster were made by dissolving between 21 and 22 mg of the solid in 0.25 ml of CH_2Cl_2 and 0.25 ml of $\text{CH}_2\text{ClCH}_2\text{Cl}$. For the preparation of the electron-beam-irradiated samples,

^{a)}Electronic mail: wybourne@oregon.uoregon.edu

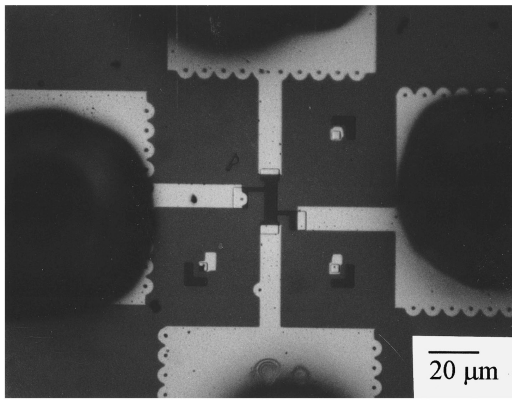


FIG. 1. Electron micrograph of the patterned gold cluster structure.

a solution was spin coated onto Si_3N_4 coated Si wafers at 1500 rpm for 25 s. The film was patterned by exposure to a 40 kV electron-beam at a line dosage of 100 nC/cm. The areas of the film not exposed to the electron-beam were removed by a CH_2Cl_2 rinse. This procedure produced well-defined structures, as shown in Fig. 1, which appeared to be smooth and continuous under inspection by SEM. Attempts were made to pattern the material using 254 nm ultraviolet (UV) lithography, but it was found to be insensitive to this wavelength. The defined structures had dimensions as small as $0.1 \mu\text{m}$ and inspection by atomic force microscopy measured the film thickness to be 50 nm. The patterned organometallic samples were spin coated with poly(methylmethacrylate) which was electron-beam exposed and developed to define contact regions. Contacts were fabricated using thermal evaporation of 100 nm of gold and conventional liftoff procedures. The nonirradiated samples were prepared by drop casting the solution onto a set of interdigitated gold electrodes on glass. The electrode separation was $15 \mu\text{m}$.

Direct current (dc) I - V measurements were made in a shielded vacuum chamber. The samples were mounted on a clean Teflon stage and were connected to a constant dc voltage source and electrometer with rigid triaxial lines. Temperature control from 195 to 350 K was accomplished by varying the temperature of an oil bath surrounding the chamber. To assist with thermal equilibration of the sample, helium exchange gas was introduced into the chamber. The helium was removed before electrical measurements were made. The data showed little temperature drift over a typical 4 h measurement sweep. The intrinsic leakage current of the apparatus was measured in the absence of a sample. It was found to be linearly dependent on bias over the range -100 to 100 V, and at 195 K had a maximum value of 60 fA. This leakage current set the minimum resolved conductance of about $10^{-15} \Omega^{-1}$, while the ultimate resolution of the current measurement was 10 fA. Constant amplitude rf signals with frequencies, f , from 0.1 to 5 MHz, were applied to the samples through a dipole antenna at 195 K. No attempt was made to optimize the coupling between the rf signal and the sample.

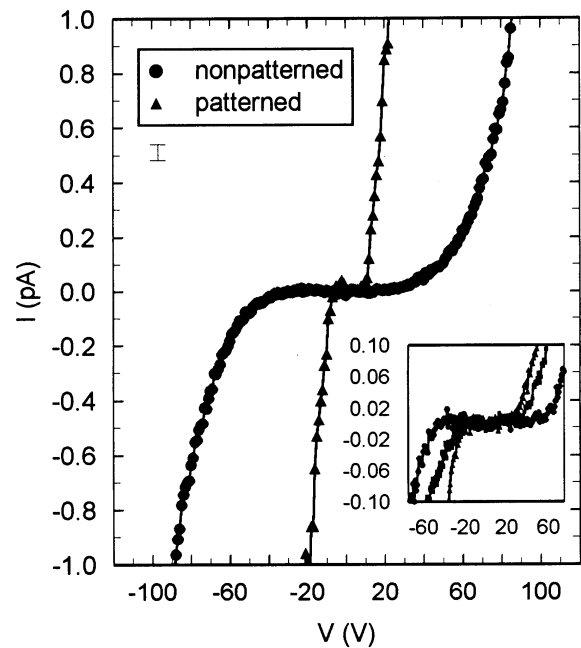


FIG. 2. The I - V characteristics for both patterned and nonpatterned samples. The data for the patterned and nonpatterned samples were taken at 195 and 300 K, respectively. The inset shows how the I - V characteristics of a nonpatterned sample change with repeated measurement.

III. RESULTS AND DISCUSSION

Both patterned and nonpatterned samples showed highly nonlinear I - V characteristics, as shown in Fig. 2. The characteristics have been corrected to account for the intrinsic leakage current of the apparatus. The electrical transport of the electron-beam-patterned sample exhibited current suppression up to a threshold voltage of magnitude 6.7 ± 0.6 V, above which the current increased abruptly. The

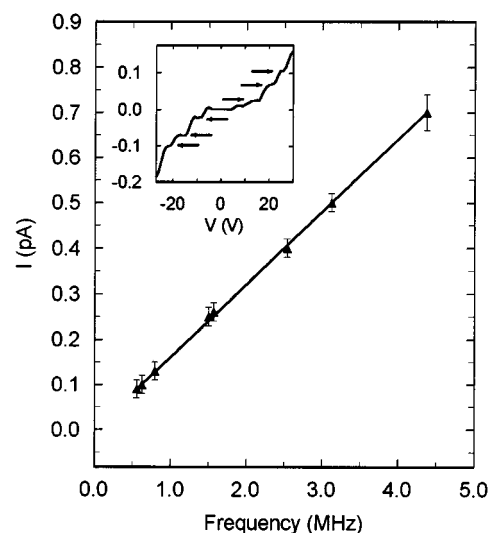


FIG. 3. The current vs frequency of the applied rf signal at which the $n/m = 1$ plateau is observed. The inset shows the plateau structure for an applied rf signal of 0.626 MHz.

magnitude of the threshold voltage did not change with time. The I - V characteristics of the nonpatterned sample also had a region of current suppression with significantly higher threshold voltages, as seen in Fig. 2. Unlike the data from the patterned sample, the threshold voltage magnitude became smaller as a function of the time the bias was applied. The changing threshold voltage is shown in the inset to Fig. 2. No changes were observed as a function of time alone. The application of a rf signal introduced plateaus in the I - V characteristics of both types of sample, as illustrated for the patterned sample in the inset to Fig. 3. The rf behavior of nonpatterned samples is still under investigation so our discussion will focus on the plateaus observed in the patterned sample characteristics. The current at which the plateaus occur was found to be proportional to the applied signal frequency. Several distinct constants of proportionality were found¹⁶ with the highest being $1.59 \pm 0.04 \times 10^{-19}$ C, as shown in Fig. 3.

Various mechanisms could account for the shape of the nonlinear I - V characteristics. These include forward biased diode behavior, variable range hopping and transport in arrays of ultrasmall metal islands, where Coulomb charging effects are dominant. The rf induced current plateaus are not expected in diode controlled transport, yet are representative of coherent tunneling in Coulomb blockade systems.⁶ Thus, observation of both suppressed current and the rf plateaus support Coulomb blockade dominated transport in an array of ultrasmall metal islands.

Transport in ordered arrays of tunnel junctions and metal islands that have tunneling resistances $> h/e^2$, and a charging energy significantly above kT has been modeled by several groups.¹⁷⁻¹⁹ In all cases it is predicted that Coulomb charging introduces a threshold voltage below which current through the array is suppressed. As the applied voltage is increased well beyond threshold, the I - V characteristic approaches a linear asymptote with a slope related to the tunnel resistance. Under the same tunnel barrier and temperature constraints, Middleton and Wingreen (MW) have discussed one- and two-dimensional arrays of maximally disordered normal metal islands, where disorder is introduced as random offset charges on each dot.²⁰ They predict current suppression below a threshold voltage, which scales with the number of junctions N along the current direction. Above threshold, the current is predicted to scale as $I \sim (V/V_T - 1)^\gamma$. Analytically, γ is 1 for one-dimensional arrays and $5/3$ for infinite two-dimensional arrays. Numerical simulations predict $\gamma = 2.0 \pm 0.2$ for finite two-dimensional arrays.²⁰ Since no attempt was made to order the gold core arrangement of either the patterned or nonpatterned samples, it is expected that a disordered model should describe the data more closely. In all cases this expectation was upheld by the behavior of the high current data, which did not approach a linear asymptote predicted for ordered systems. Instead, the high current data scaled as predicted for disordered systems. For the electron-beam patterned sample $\gamma = 1.6 \pm 0.2$, and for the nonpatterned samples $\gamma = 2.1 \pm 0.3$, as shown in Fig. 4. These results are consistent with both types of sample being

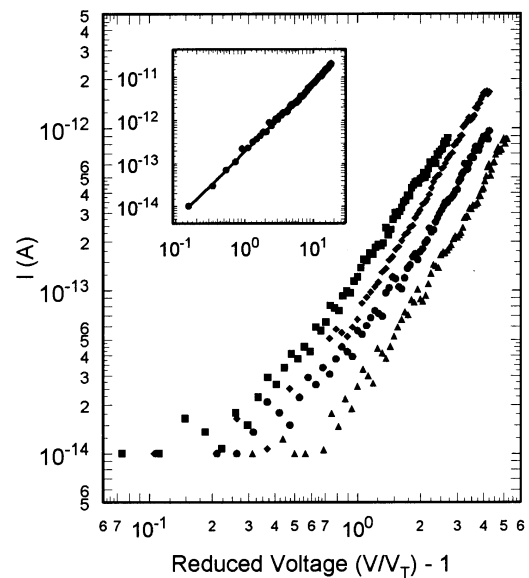


FIG. 4. The current vs reduced voltage for repeated sweeps of a nonpatterned sample at 300 K. The average slope at high current is 2.1 ± 0.3 . The turnover at low current is a result of the 10 fA minimum current resolution of the apparatus. The inset shows the current vs reduced voltage for a patterned sample at 195 K.

disordered two-dimensional arrays. For all sets of data, the threshold voltages obtained from the scaling are consistent with the values estimated directly from the I - V data.

The introduction of plateaus in the patterned sample I - V characteristics is similar to the rf response reported in other Coulomb blockade systems.^{21,22} This effect has been attributed to phase locking of single electron tunneling events by the external rf signal.⁶ When the n th harmonic of the applied frequency corresponds to the m th harmonic of the frequency of tunneling in the system, mI/e , the current becomes locked to a value $I = (n/m)ef$. Therefore, the linear relationship shown in Fig. 3 suggests that correlated tunneling is present in the samples. The observation of other rational fractions n/m is indicated on the inset to Fig. 3, and has been discussed elsewhere.¹⁶

The patterned samples had stable I - V characteristics with time and temperature. Furthermore, as the temperature was raised above about 250 K the I - V characteristics developed almost linear behavior up to V_T . The conductance below V_T was activated, with activation energies E_A in the range 30–70 meV. One method to estimate the charging energy from the activation energy is to use the argument that the charging energy for one island in a infinite two-dimensional array, $E_C \approx 4E_A$.²³ This argument was developed to explain similar activated behavior observed in tunnel junction systems at low temperatures. Assuming current suppression requires $E_C \geq 10kT$, the sample with the largest activation energy should develop a Coulomb gap below ~ 300 K. This value is within a factor of 2 of the measured temperature at which clear blockade behavior occurs in the patterned samples. Given the accuracy to which E_C is known, the temperature dependence of the conductance within the Coulomb gap is consistent with the observation of blockade behavior.

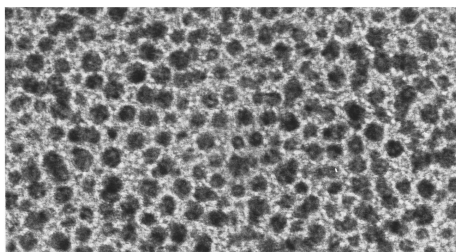


FIG. 5. A TEM micrograph of a self-assembled, biphenylmercaptan stabilized Au_{55} array. The magnification is 1 M.

Using this value of E_c , the effective capacitance of a metal core in the patterned array is $3 \times 10^{-19} < C < 7 \times 10^{-19}$ F. These values are close, but larger than the classical geometric capacitance of an isolated Au_{55} cluster $C = 4 \pi \epsilon \epsilon_0 r \approx 2 \times 10^{-19}$ F, where the dielectric constant of the surrounding ligand shell ϵ is expected to be ~ 3 . The agreement between the two estimates of capacitance supports the notion that the current suppression in the metal cluster arrays is due to charging of individual Au_{55} clusters.

Having established the capacitance of each core some constraints on the number of Au_{55} cores that make up the patterned array, can be obtained from the measured threshold voltage and rf data. From the predicted threshold voltage in a disordered array, $V_T = \alpha Ne/C$,²⁰ where α is a parameter between 0 and 0.5 that depends on the ratio of the capacitance between cores to the capacitance to a ground plane. We find αN to be ~ 10 . Unfortunately, it is not possible to determine N because we do not have enough structural information about the sample to estimate α reliably. Given the constraint that steps in the $I-V$ characteristics are only found when $f < 0.1/(R_T C)$,⁶ the fact that steps are seen up to $f = 5$ MHz gives the upper limit $R_T < 1 \times 10^{11} \Omega$. The differential resistance obtained from the $I-V$ characteristic well above threshold is anticipated to be $R_{\text{diff}} \sim (N/M)R_T$, where M is the number of parallel channels in the array. This estimate yields $N/M \geq 30$. From the delineated sample dimensions and the size of an individual cluster, a close packed array would have $N/M \sim 5$. The large difference between the expected and experimentally derived values of N/M suggests that the full width of the sample is not involved in transport. One explanation for the discrepancy in N/M may be that many of the gold cores coalesce during sample fabrication, so that individual clusters between larger regions of gold dominate the transport.

One major difference between the two types of sample studied is the long-term stability of the transport characteristics of the electron-beam-irradiated samples compared with the nonirradiated samples. A second difference is that blockade behavior in the nonpatterned samples persists up to at least RT. We believe the transport in both cases is dominated by charging of single Au_{55} cores; and that the enhanced stability of the patterned samples comes from a more rigid structure created by electron-beam irradiation. Details of the electron-beam interaction with this organometallic material have yet to be determined. Particularly important will be an understanding of the cross-linking mechanism, and the pos-

sibility that the electron-beam exposure may cause the gold core coalescence that appears to occur. However, it is clear that electron-beam exposure produces some form of cross-linking, which effectively locks the metal cores in place creating a stable arrangement whose transport characteristics show Coulomb blockade effects close to RT.

One potential cause of instability in the $\text{Au}_{55}[\text{P}(\text{C}_6\text{H}_5)_3]_{12}\text{Cl}_6$ structures is the lability of the triphenylphosphine ligand shell.²⁴ Recently, we have prepared thiol stabilized Au_{55} clusters (Au_{55} surrounded by ~ 25 alkyl or aryl thiolate ligands) that self-assemble into close-packed ordered arrays, as shown in Fig. 5.²⁵ From UV visible spectroscopy studies, these clusters exhibit dramatically improved thermal stability. Compared to the $\text{Au}_{55}[\text{P}(\text{C}_6\text{H}_5)_3]_{12}\text{Cl}_6$ clusters that decompose within ~ 1.5 h, the thiol stabilized clusters exhibit no decomposition after 24 h under the same conditions.²⁵ How this improved thermal stability will influence the electrical stability of a nonirradiated, self-assembled sample is unknown at this time. Another advantage of the thiol ligand shell is that it can be used to bond the cluster covalently to a rigid molecular scaffold to form ordered one-dimensional arrays. Work is in progress toward the fabrication of and transport measurements on such ordered one-dimensional arrays. The details will be presented elsewhere.²⁶

ACKNOWLEDGMENTS

This work was partially supported by the Office of Naval Research under Contract Nos. N00014-93-0618 and N00014-93-1-1120. One of the authors (L.C.) acknowledges support from the Department of Education.

- ¹J. Peretz and L. W. Swanson, *J. Vac. Sci. Technol. B* **10**, 2695 (1992).
- ²L. R. Harriot, K. D. Cummings, M. E. Gross, and W. L. Brown, *Appl. Phys. Lett.* **49**, 1661 (1986).
- ³T. K. Stark, T. M. Mayer, D. P. Griffins, and P. E. Russell, *J. Vac. Sci. Technol. B* **9**, 3475 (1991).
- ⁴P. Hoffmann, G. B. Assayag, J. Gierak, J. Flicstein, M. Maar-Stumm, and H. van den Bergh, *J. Appl. Phys.* **74**, 7588 (1993).
- ⁵M. Yan, S. X. Cai, J. C. Wu, C. A. Duchi, M. Kanskar, M. N. Wybourne, and J. F. W. Keana, *Polym. Mater. Sci. Eng.* **70**, 36 (1994).
- ⁶D. V. Averin and K. K. Likharev, in *Mesoscopic Phenomena In Solids*, edited by B. Al'tshuler, P. Lee, and R. A. Webb (Elsevier, Amsterdam, 1991).
- ⁷G. Schön and U. Simon, *Colloid Polym. Sci.* **273**, 101 (1995).
- ⁸R. P. Andres, T. Bein, M. Dorogi, S. Feng, J. I. Henderson, C. P. Kubiak, W. Mahoney, R. G. Osifchin, and R. Reifenberger, *Science* **272**, 1323 (1996).
- ⁹A. J. Rimberg, T. R. Ho, and J. Clarke, *Phys. Rev. Lett.* **74**, 4714 (1995).
- ¹⁰K. K. Likharev, in *Granular Nanoelectronics*, edited by D. K. Ferry, J. R. Barker, and C. Jacoboni (Plenum, New York, 1991), p. 371.
- ¹¹J. R. Tucker, *J. Appl. Phys.* **72**, 4399 (1992).
- ¹²A. P. Alivistos, K. P. Johnson, X. Peng, T. E. Wilson, C. J. Loweth, M. P. Bruchez, Jr., and P. G. Schultz, *Nature (London)* **382**, 609 (1996).
- ¹³R. P. Andres, J. D. Bielefeld, J. I. Henderson, D. B. Janes, V. R. Kolagunta, C. P. Kubiak, W. J. Mahoney, and R. G. Osifchin, *Science* **273**, 1690 (1996).
- ¹⁴D. L. Feldheim, K. C. Grabar, M. J. Natan, and T. E. Mallouk, *J. Am. Chem. Soc.* **118**, 7640 (1996).
- ¹⁵G. Schmid, *Inorg. Synth.* **27**, 214 (1990).
- ¹⁶L. Clarke, M. N. Wybourne, M. Yan, S. X. Cai, and J. F. W. Keana, *Appl. Phys. Lett.* **71**, 617 (1997).
- ¹⁷N. S. Bakhvalov, G. S. Kazacha, K. K. Likharev, and S. I. Serdyukova, *Sov. Phys. JETP* **68**, 581 (1989).

- ¹⁸N. S. Bakhvalov, G. S. Kazacha, K. K. Likharev, and S. I. Serdyukov, *Physica B* **173**, 319 (1991).
- ¹⁹U. Geigenmüller and G. Schön, *Europhys. Lett.* **10**, 765 (1989).
- ²⁰A. A. Middleton and N. S. Wingreen, *Phys. Rev. Lett.* **71**, 3198 (1993).
- ²¹L. J. Geerligs, V. F. Anderegg, P. A. M. Holweg, J. E. Mooij, H. Pothier, D. Esteve, C. Urbina, and M. H. Devoret, *Phys. Rev. Lett.* **64**, 2691 (1990).
- ²²P. Delsing, K. K. Likharev, L. S. Kuzmin, and T. Claeson, *Phys. Rev. Lett.* **63**, 1861 (1989).
- ²³T. S. Tighe, M. T. Tuominen, J. M. Hergenrother, and M. Tinkam, *Phys. Rev. Lett.* **47**, 1145 (1993).
- ²⁴G. Schmid, *Chem. Rev.* **92**, 1709 (1992).
- ²⁵L. O. Brown and J. E. Hutchison (unpublished).
- ²⁶L. O. Brown, J. E. Hutchison, L. Clarke, and M. N. Wybourne (unpublished).